ORIENTATIONAL CHANGES OF THE ABSORBING DIPOLE OF RETINAL UPON THE CONVERSION OF RHODOPSIN TO BATHORHODOPSIN, LUMIRHODOPSIN, AND ISORHODOPSIN

M. MICHEL-VILLAZ, C. ROCHE, AND M. CHABRE
Laboratoire de Biologie Moléculaire et Cellulaire (E.R. 1gg du CNRS), Département de Recherche Fondamentale, Centre d'Etudes Nucleaires de Grenoble, 85 X, 38041 Grenoble, France

ABSTRACT The orientational change of the absorbing dipole of the retinal chromophore in vertebrate rhodopsin (rhodo) upon photo-excitation to bathorhodopsin (batho), lumirhodopsin (lumi) and isorhodopsin (iso), has been studied by polarized absorption and linear dichroism measurements on magnetically oriented frog rod suspensions that were blocked at liquid nitrogen temperature. Both the azimuthal component $\Delta\theta$ and the polar component $\Delta\phi$ of the total angular change were studied in separate experiments. $\Delta\theta$ was estimated from polarized absorption measurements on rods oriented transversally with respect to the analyzing beam. The data show unequivocally that upon the rhodo → batho transition, the dipole shifts out of the membrane plane by only a few degrees: $\Delta\theta \simeq -3°$. This azimuthal shift was nearly exactly reversed upon the batho → lumi decay. A very small shift ($\Delta\theta \leqslant 1°$) toward the membrane plane was observed upon a rhodo → iso conversion. The polar component $\Delta\phi$ of the angular shift was estimated by studying the photoreversion of linear dichroism induced by photo-excitation with polarized light in rods oriented parallel to the analyzing beam. Upon the rhodo → batho transition, there was a shift $\Delta\phi = 11 \pm 3°$. The overall angular shift upon this first photo-exciting step, which corresponded to the isomerisation of retinal, was only $\Delta\Omega = 11 \pm 3°$. This is smaller than what may be expected for a *cis-trans* isomerization of a retinal molecule with one end fixed, and different from what has been previously estimated by another group. These discrepancies are discussed.

INTRODUCTION

Illumination of visual rhodopsin initiates in the pigment molecule, a sequence of reactions identified through large spectral absorbance changes of the retinal chromophore. Only the first step, characterized by a large bathochromic shift, is light dependent; the subsequent reactions result from decay in the dark of this initial photoexcited state, bathorhodopsin (batho).[1] This initial step is stable at liquid nitrogen temperature. Inasmuch as the retinal chromophore is in the 11-*cis* conformation in native rhodopsin and is extractable in the all-*trans* conformation from the late decay products, it was proposed more than 20 years ago (Hubbard and Kropf, 1958; Yoshizawa and Wald, 1963) that the only effect of light was to isomerize retinal in the initial transition rhodopsin (rhodo) → batho. This was supported by a large variety of experiments, and was widely accepted. No direct proof of the all-*trans* conformation of retinal in batho was provided, however, as the chromophore cannot be extracted from this transient state. The dogma was challenged in 1977 when picosecond techniques demonstrated that the transition rhodo → batho is completed within a few picoseconds, even at liquid helium temperature. This, it was claimed, was too short a time for an isomerization to take place. An alternative hypothesis was that the initial photoexcitation only induced a proton translocation along the polyene chain of the retinal (Peters et al., 1977). Because of this proposal, new studies on bathorhodopsin were begun. One type of approach was to study the formation of bathoproducts by irradiating rhodopsin reconstituted with chemically modified retinal, or with isomers of retinal that had conformation different from the normal 11-*cis* conformation. It was demonstrated, for example, that the same batho is obtained when isorhodopsin (iso) is illuminated. Iso contains 9-*cis* retinal as its chromophore and has kinetics on the order of picoseconds (Green et al., 1977). This demonstrated that an isomerization could occur on this time scale, since to reach a common intermediate, when starting from two pigments with different chromophore conformations, one has to pass through an isomerization at least on one side.

[1] *Abbreviations used in this paper:* rhodopsin, rhodo; bathorhodopsin, batho; isorhodopsin, iso; lumirhodopsin, lumi; metarhodopsin, meta; linear dichroism, LD; rod outer segment, R.O.S.

Another extensively investigated approach has been Raman resonance spectroscopy. The analysis of Raman spectra is neither straightforward nor always unambiguous. Recent work, however, using rhodopsin reconstituted with synthetic retinal molecules deuterated specifically at various positions, seems to demonstrate convincingly that the conformation of retinal in batho is indeed of the all-*trans* type, but rather distorted (Eyring et al. 1980).

Compared with the abundant literature on sophisticated rapid kinetics and Raman spectroscopy, it seems surprising that only one group has studied a spectroscopic parameter in batho and other early intermediates, which seems directly related to the geometry of the retinal molecule; that is, the orientation of its main absorbing dipole in the visible. Dipolar absorption is highly anisotropic and in retinal the direction of anisotropy is geometrically related to that of the conjuguated double-bond system of the polyene chain. In the all-*trans* conformation the absorbing dipole is aligned with the straight polyene chain. A *cis-trans* isomerization changes the geometry of the chain and should induce a change of orientation of this absorbing dipole. The direction of preferential absorption in rhodopsin *in situ* is defined with respect to the disk membrane plane by its two spherical angles θ and ϕ (Fig. 1). At room temperature the rhodopsin molecules are free to rotate in the membrane, but the azimuthal angle θ remains fixed and is defined with respect to the rod axis in an intact organelle; it is measurable by polarized absorption microspectroscopy (Liebman, 1962, 1972; Harosi, 1975). In native rhodopsin, the value of θ is $\sim 72°$, which means that the chromophore is almost lying in the membrane plane; the angle between the chromophore and the disk membrane plane is often quoted in the literature as $\pi/2 - \theta$, which is therefore $\sim 18°$. The polar angle ϕ cannot be defined because the rhodopsin molecules rotate freely in the membrane plane. This rotation can be blocked by cooling to liquid nitrogen temperature. The rhodopsin molecules are then fixed, but their polar orientation is randomly distributed and ϕ is still undefined because of the lack of an internal reference frame within each rhodopsin molecule. However, by bleaching those immobilized rhodopsin molecules with linearly polarized light, a population can be photoselected with a preferential polar orientation of the absorbing dipole. On such a photoselected population an eventual change, $\Delta\phi$, of the polar orientation of the chromophore upon a subsequent photoexcitation is measurable. From measurements of $\Delta\theta$ and $\Delta\phi$ the overall orientational change of the dipole, $\Delta\Omega$, upon a given transition can be deduced (see Fig. 1).

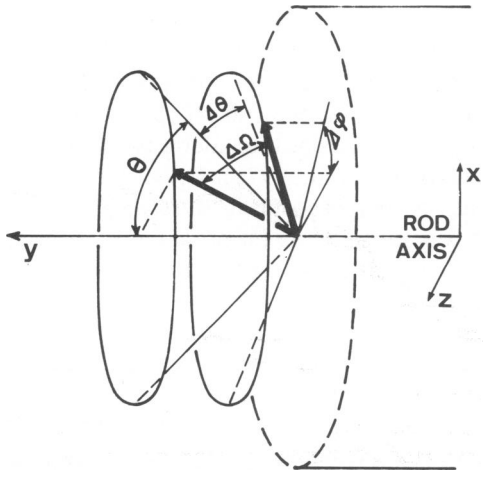

FIGURE 1 Geometry of the absorbing dipole of the chromophore. At liquid nitrogen temperature, the rotational motion is blocked and ϕ is fixed. The reorientation angle $\Delta\Omega$ upon a transition such as rhodo → batho is defined by its azimutal component $\Delta\theta$ and its polar component $\Delta\phi$.

Such types of measurements have been performed only by the Yoshizawa group (Tokunaga et al., 1976; Kawamura et al., 1977, 1978, and 1979). They obtained an estimate of $\Delta\theta$ from experiments based on the comparison of the absorption changes, upon the rhodo → batho transition, in various types of samples (solution of rhodopsin in digitonin, unoriented suspensions of R.O.S., and retinas). Their result indicated that upon the rhodo → batho transition, the chromophore shifts towards the membrane plane by about 20°, so as to lie exactly in this plane in batho. From photoselection experiments on retinas, they estimated the polar rotation $\Delta\phi$ in the same transition to be also of the order of 20°. This gave an overall reorientation angle $\Delta\Omega = 26°$, which is quite a large value, and would indicate that the isomerization involves a substantial movement of the chromophore in the fixed rhodopsin molecule.

The method of the Yoshizawa group was mostly based on absorption measurements with unpolarized light, and involved the comparison of spectra obtained with various types of preparations. We have examined the same problem with a different experimental approach: our methods are based on the preparation of magnetically oriented samples of R.O.S., blocked at liquid nitrogen temperature, and on combined absorption and linear dichroism measurements performed simultaneously or sequentially on the same sample, or samples of the same type, with the same optical equipment. The high sensitivity of the linear dichroism measurements and the possibility that we have to align the rods in a direction perpendicular to that of the analyzing beam allow sensitive measurements of $\Delta\theta$ and $\Delta\phi$ and provide a large variety of controls with different geometries of orientation or of photoexcitation. Although we do find an orientational change upon the rhodo → batho transition, our result differs notably from that of the Yoshizawa group. We demonstrate in particular that the dipole shifts not toward the membrane plane, but farther out of this plane, and by only a small angle. A definite but small polar rotation is also observed. This combines to give an overall orientational change not greater than 13°. The measurements have also been extended to iso and the later decay product lumirhodopsin (lumi).

MATERIAL AND METHODS

All preparations and measurements are performed in total darkness or under dim red light, unless stated otherwise. The preparation of magnetically oriented samples of isolated R.O.S. at room temperature has already been described in previously published work from this laboratory (Chabre, 1975; Chabre and Breton, 1979) but the making of oriented samples at liquid nitrogen temperature requires a special procedure.

Sample Preparation

Samples of various concentrations were required for different measurements, but the procedure was always the same: only the number of retinas varied.

In a typical experiment the R.O.S. are extracted from three frog (*Rana esculenta*) retinas by shaking in standard Ringer solution and sedimented at low speed according to our standard procedure (Chabre, 1975). The Ringer composition is (in mM): NaCl 101.8, KCl 12.7, $MgCl_2$ 2.1, $CaCl_2$ 1.9, Tris acetate buffer 10, pH adjusted to 7.4. The supernatant is removed and the rods are resuspended in 400 μl of Ringer-glycerol mixture 3 : 7 vol/vol, and stirred with a spatula for ~30 s to insure an homogeneous dispersion of the rods in the viscous glycerol medium. The suspension is then transferred into a specially designed sample cell of 4-mm optical path length and ~1-cm^2 area. The body of the cell is made of transparent lucite so that the sample may also be illuminated perpendicularly to the optical axis. The windows are made of 0.5-mm thick altuglass 218. The cell has two copper flanges on the front and the back, for cooling, and is fitted with a 100-Ω platinum resistance to measure the sample temperature. The shape of the cell and its complete filling without any bubbles are critical for the optical quality and the orientation of the frozen samples, as discussed below. The sample cell was ready for orientation and cooling within 10 min from the separation of the R.O.S. from the retina, and within 5 min from mixing with glycerol. We had observed in previous experiments at room temperature (Chabre and Breton, 1979) that good linear dichroism spectra were obtained in glycerol-water mixtures after this short delay and that on longer delays the rod shape tended to deteriorate. The orientation and cooling procedure was therefore started as soon as the sample was ready.

Magnetic Orientation and Cooling

At room temperature and in Ringer solution, a magnetic field intensity of the order of 10 kgauss (kG) is sufficient to obtain a perfect orientation of the rods (Chabre and Breton, 1979). With addition of glycerol and cooling, two types of problems are encountered. First, there is a disorientation due to convection movements in the cooling glycerol solution, which becomes very viscous before freezing at ~ -100°C. Second, cracks and optical defects appear upon freezing. There are three solutions to these problems: (*a*) a cell shape which minimizes the effects of convection currents, (*b*) a careful control of the cooling program, and (*c*) an increase of the orienting magnetic field. (*a*) led us to design cells of nearly square cross section, although we avoided sharp corners which would favor the formation of cracks. This shape also provided a better side window for lateral illumination. For (*b*), our empirical conclusion is that one must cool slowly and regularly at ~10°C/min down to -110°C and then cool very fast by plunging the sample directly into liquid nitrogen; this procedure gave a very high proportion of samples without any cracks. For the field strength, a first set of experiment used the 15-kG field of an electromagnet in our laboratory. This gave samples with a good degree of orientation but the direct microscopic observation of the rods in the sample at liquid nitrogen temperature showed that it was not always perfect; in particular, with sample cells which were originally of an elongated shape, a systematic effect of convection currents was detectable, both through the microscopic observation and through a residual dichroism measured on samples in which the rods were oriented parallel to the optical beam of the spectrometer (for axial orientation in our nomenclature, see Fig. 4). To eliminate this we changed the cell shape, as explained above, and used for orientation very high magnetic fields which were available to us in a nearby physics institute (Service National des Champs Intenses du Centre National de la Recherche Scientifique). The magnet was of the Bitter type, not supraconducting, with a maximum field of 170 kG in a 50-mm Diam bore-hole. It could be switched on or off within a minute, which is very convenient for our preparations. With such a high field, perfectly oriented samples were consistently obtained. Microscopic controls showed the rod and rod fragments to be all perfectly aligned over the full area of the sample. Some of the rods, however, were slightly curved, an effect probably due to the glycerol before the cooling. Part of the data presented have, however, been obtained with the low-field orientation, which gave results entirely compatible with that of the high-field orientation.

In both types of magnet the procedure was as follows: the sample cell is fitted in a copper holder inserted inside a cylindrical Dewar installed in the magnet. The cell could be oriented so that its optical axis was either parallel or perpendicular to the magnetic field direction. As the rods align parallel to the field, this gave a sample with "axial" and "transverse" orientation according to our nomenclature (Fig. 4). The magnetic field was switched on while the sample was at room temperature. Then the sample was cooled at the appropriate speed by raising slowly the level of the liquid nitrogen which was in contact with the copper holder at the bottom of the Dewar. When the cooling procedure was terminated, the field was switched off and the frozen sample was rapidly transferred into another Dewar where it could be preserved indefinitely under liquid nitrogen.

More than 20 oriented samples were prepared, which were of very good optical quality, with no crack on an area larger than that of the beam spot (about 4-mm wide and 6-mm high).

Sample Geometry and Illumination Geometry

For measurements, the sample was transferred into a Dewar equipped with four windows which was installed on the optical bench of the dichrograph (Fig. 2). The sample was fixed into a copper holder which was in contact with the liquid nitrogen at the bottom of the Dewar. The orientation axis of the rods was set either parallel to the optical axis in the axial geometry, or perpendicular to the optical axis and horizontal in the transverse geometry. At liquid nitrogen temperature, where the rotational freedom of the rhodo molecules is blocked, any illumination from a given direction creates, even with unpolarized light, an anisotropically photoselected population of batho, unless the direction of illumination coincides with the rod axis. Even on a randomly dispersed rod suspension this photoselection occurs, since the illumination is never isotropic. The only way to avoid such a photoselection is to orient the rods and illuminate them in the direction of orientation. Unless one wants specifically to create a photoselected population, transversally oriented rods have to be illuminated transversally.

For illumination we used a 250-W slide projector equipped with a condenser, a mechanical shutter, and a light guide. The light can be directed onto the sample either axially through the frontal window with the help of a removable 90° deflection prism or transversally through the lateral window. Both windows can be equipped with suitable filters and polarizers when necessary.

Photoexcitation and Photoregeneration, Rhodopsin $\rightleftharpoons$ Batho $\rightleftharpoons$ Iso Equilibria and Lumirhodopsin

At liquid nitrogen temperature, illumination of rhodo produced stable batho, but photoreversal reaction on batho led also partially to iso and photoequilibria between the three states rhodo $\rightleftharpoons$ batho $\rightleftharpoons$ iso was reached. It is only in the initial dark-adapted state that one has pure rhodo. For photoexcitation we used an interference filter with peak transmittance at 472 nm. That is near the maximum absorbance of iso. A photostationary state with a large amount of batho and a minimal

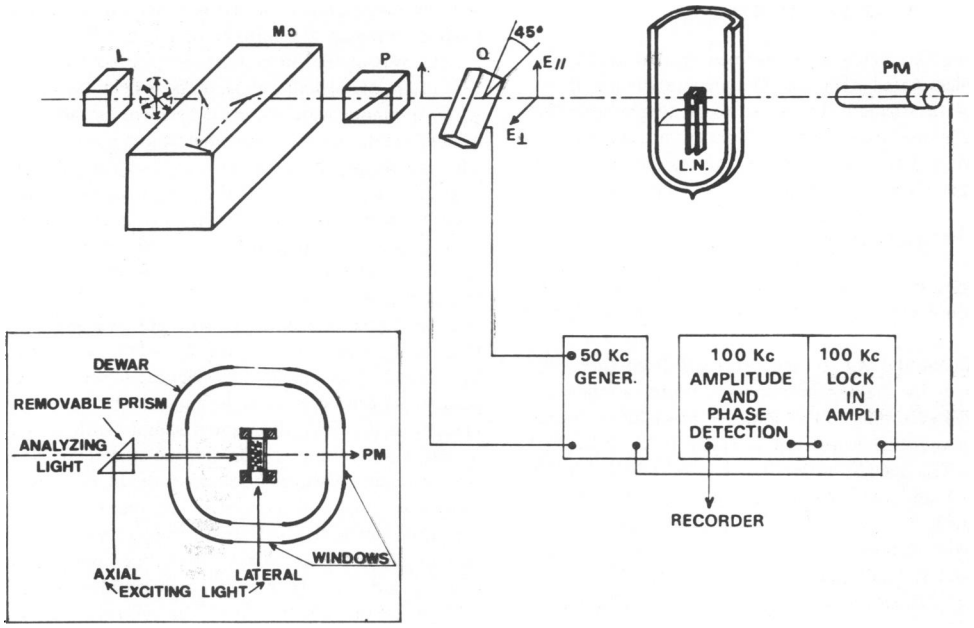

FIGURE 2 Scheme of the linear dichrograph with a transversally oriented sample blocked at liquid nitrogen temperature. L, light source; Mo, monochromator; P, polarizer; Q, quartz modulator; L.N., liquid nitrogen; PM, photomultiplier. *Inset,* top view of the geometry of orientation and illumination of the rods. The rods can be oriented either transversally (as shown) or axially.

contamination of iso was reached within 5 min of illumination through this filter. Since batho absorbs at wavelengths much longer than the two other states, it can be totally eliminated by photoreversal with long-wavelength light. For photoreversal we used a red filter cutting off wavelength below 610 nm (Wratten 29) and complete photoreversion was reached within 30 s of illumination.

This photoregenerated state always contains an admixture of iso. When performing repetitive experiments on the same sample with a photoregeneration cycle one has to know the proportion of iso in the photoregenerated state. This was estimated to 25% by comparison with the state containing the maximum amount of iso. This state was obtained by illuminating at saturation (≃15 min) with a filter cutting off wavelengths <580 nm (Wratten 23 A). Lumi was obtained by letting the sample warm up to −120°C for 20 min after saturating illumination with the 472-nm interference filter at liquid nitrogen temperature. The measurements were performed after returning the sample to liquid nitrogen temperature. Photoreversion from lumirhodopsin was obtained by a sequence of 10-min illumination with the interference filter (I_{472} nm) and 30 s with the red filter.

Linear Dichroism Measurements

The linear dichrograph is a modified version of that used in previously published work (Chabre and Breton, 1979). It is based on the use of a photoelastic modulator [Morvue PEM FS3] vibrating at 50 kcycle frequency, which produces linearly polarized light alternatively in the vertical and in the horizontal direction. Behind the photomultiplier a selective amplifier, locked on the quartz oscillator frequency, detects a signal proportional to the difference of absorbance of the sample for the two orthogonal directions of polarization. The photomultiplier gain has a feedback control by its total current to compensate for the wavelength dependence of the sample transmission and of the efficiencies of the different components of the apparatus. For samples of low optical densities, the exponential absorbances $e^{-A_\parallel}$ and $e^{-A_\perp}$ are well approximated by their first-order developments: $e^{-A} \simeq 1 - A$ and the measured difference is proportional to the linear dichroism amplitude: $LD = A_\parallel - A_\perp$. The system has a very high sensitivity, and is, therefore, best suited for samples of low optical densities. In linear dichroism measurements, most of the light-scattering effects are eliminated, and the base lines are perfectly flat outside the dichroic bands. This has already been discussed in previous papers (Chabre and Breton, 1979; Breton et al. 1973).

Linear dichroism spectra of transversally oriented rods are shown on Fig. 3. In this geometry, a linear dichroism spectrum has the same wavelength-dependent shape as for an absorption spectra, but its amplitude depends on the angle θ.

The scanning speed was of 5 or 10 nm/s. The cross section of the light beam on the sample is of 4 × 6 mm^2. This large cross section allows the use of light flux small enough so that the bleaching by the measuring beam was undetectable upon repetitive scanning of the full spectrum.

Axially oriented samples are not dichroic. Photoexcitation by linearly polarized light can, however, induce linear dichroism by photoselection in such samples.

Absorbance Measurements

The absorbance measurements were performed on the same apparatus. The photoelastic modulator and the photomultiplier gain control were switched off. We measured then the current of the photomultiplier at fixed voltage, as on a single beam spectrometer. The base line was distorted because of the wavelength dependence of the monochromator and photomultiplier efficiencies; the analysis is based on difference spectra which eliminate this base-line distortion.

On transversally oriented samples, absorbance was highly dependent on polarization. The monochromator always introduces a wavelength-dependent partial polarization, which cannot be eliminated. The best solution is then to fully polarize the beam, in the direction parallel or perpendicular to the orientation axis of the sample. To obtain the same light intensity for vertical and horizontal polarization direction, we needed two polarizers: a first polarizer oriented at 45° from the vertical and a second polarizer, which could be oriented vertically or horizontally. For transversally oriented samples, we call $A_\parallel$ the absorbance measured with light polarized vertically; i.e., parallel to the disk membrane plane, and $A_\perp$ that measured with horizontally polarized light.

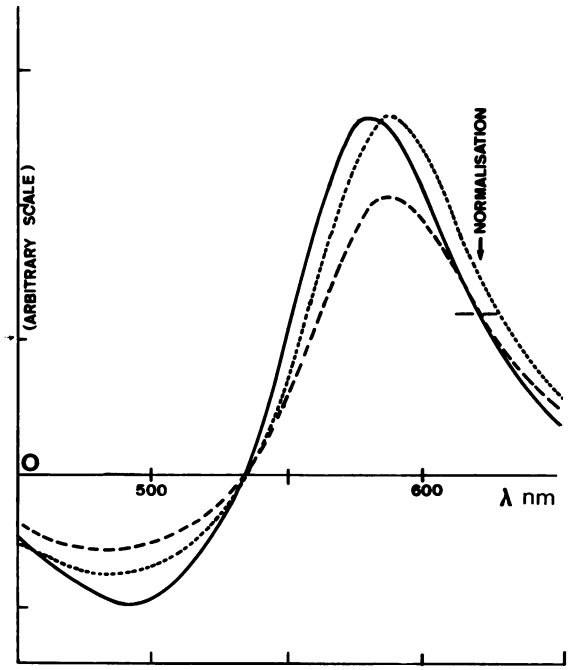

FIGURE 3 Comparison of the shape of difference spectra obtained on transversally oriented samples with that obtained on axially oriented samples for the rhodo → batho transition. For the transverse sample (—) $\Delta A_{\parallel} + \Delta A_{\perp}$ approximates closely a difference spectrum obtained with unpolarized light. For axially oriented sample ΔA is independent of the polarization, and has the same shape as the linear dichroism spectrum induced by photoselection with polarized light ΔL_{PS} (Fig. 4, geometry IV). If the spectral shapes $\epsilon_R(\lambda)$ and $\epsilon_B(\lambda)$ were not distorted, these difference spectra which have the same crossover point should be identical in shape. This is clearly not the case, whether one normalizes on the maximum amplitude (----) (as done by Tokunaga et al., 1976, their Fig. 1) or one normalizes at 620 nm (—), batho alone absorbs, (as done in Fig. 9): the difference of shapes is evident even in the spectral region where only batho absorbs. This indicates that in the axially oriented sample there is an important distortion of the spectral shapes by sieve effect.

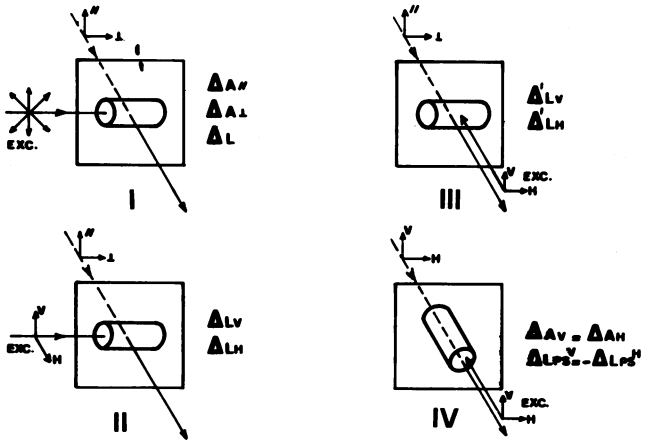

FIGURE 4 The various geometries of orientation and photoexcitation and the corresponding measurements. The geometries are mentioned by their numbers I to Q in the text.

Combined Absorbance and Linear Dichroism Measurements

The absolute accuracy of the absorbance measurement is of the order of 10^{-2} OD with our single-beam system. To get reasonable accuracy we then had to use samples having OD $\geq$ 0.1. This was too large an OD to get good responses in the LD mode (the apparatus measuring directly $e^{-A_{\parallel}} - e^{-A_{\perp}}$). There was no way to calculate exactly the exponentials when the first-order approximation was not valid, and the LD amplitudes were not strictly proportional to $A_{\parallel} - A_{\perp}$. We checked however that these distortions did not influence significantly the isosbectic point between two species such as rhodo and batho, when varying the OD of the sample from 10^{-2} to 3.10^{-1}. We could then compare directly the isosbectic points for $A_{\parallel}$, $A_{\perp}$ and LD on a single sample, in the same geometry. For comparing the shape of the difference spectra over the full wavelength range, however, we used samples of OD $\simeq$ 0.2 for the absorbance measurements and samples of OD $\simeq$ 0.02 for the LD measurements.

Selection of the Geometries for the Various Measurements

The different possible geometries of orientation and of photoexcitation are shown on Fig. 4 and the formulas necessary for the evaluations of the measurements are developed at the end of this section. There are many different possible measurements which are sensitive to $\Delta\theta$ and $\Delta\phi$. We have selected two main experiments to estimate $\Delta\theta$ and $\Delta\phi$ separately, each experiment being sensitive to only one of these parameters. Two other measurements have been performed, in which both $\Delta\theta$ and $\Delta\phi$ interfere. It is difficult to analyze in these complementary experiments the separate contributions of $\Delta\theta$ and $\Delta\phi$, but they provided overall checks of the results of the previous measurements, of the orientation of the sample, and geometry of illumination and detection.

The specific absorbance of the chromophore will be denoted $\epsilon_R(\lambda)$ for rhodo, $\epsilon_B(\lambda)$ for batho and so on. It is worth stressing that these quantities represent the absorbance of randomly oriented chromophores and that, when the chromophores are rigidly blocked at low temperature, any photoexcitation may create an anisotropy in an initially isotropic sample.

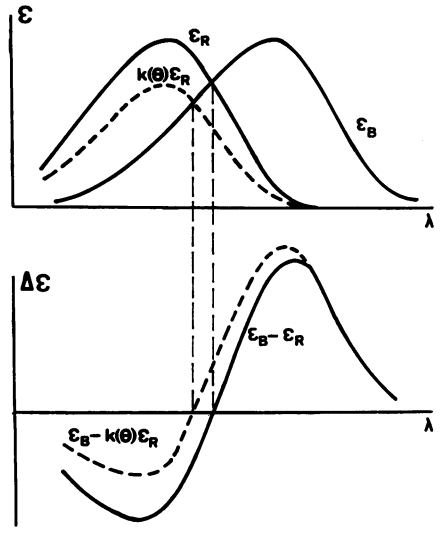

FIGURE 5 Analysis of difference spectra. Effect of the relative angular weight factors of two spectral states in a given measurement on the difference spectra for various measurements ($\Delta A_{\parallel}$, $\Delta A_{\perp}$, and ΔL) on the same transition depends only on the angular factors symbolized by k (θ). This splitting is sensitive to very small angular changes when the spectral shapes are very close.

Measurement of $\Delta\theta$: Difference Spectra Analysis

The geometry is that of type I on Fig. 4: transversally oriented rods and transverse unpolarized photoexcitation along the rod axis. The photoexcitation is, therefore, isotropic with respect to the rod axis.

Three types of measurements were performed: absorbance with light parallel to the disk membrane plane $A_{\parallel}(\lambda)$, absorbance with light perpendicular to the disk membrane plane $A_{\perp}(\lambda)$ and linear dichroism LD (λ). These three spectra were recorded before and after the transition between the two states. For the rhodo $\rightarrow$ batho transition, for example, they were recorded before and after photoexcitation at 472 nm. Difference spectra were plotted for each of the three types of measurements: $\Delta A_{\parallel}$, $\Delta A_{\perp}$, and ΔL. Because the photoexcitation in this geometry is isotropic, only θ appears in Eqs. 1, 2, and 3, which describe these difference spectra. If for example $\theta_R = \theta_B$, one sees that the wavelength dependence is given in all cases by $\epsilon_B(\lambda) - \epsilon_R(\lambda)$ which means that the three difference spectra have the same shape and in particular the same crossover point. The crossover point of a difference spectrum is the isosbectic point between the two spectral species. Our analysis is concentrated on the wavelength positions, and differences in position of these crossover points or isosbectic points, which are very insensitive to eventual spectral distortions.

If $\theta_B < \theta_R$, in Eq. 2 for $\Delta A_{\parallel}$, the weight of $\epsilon_R(\lambda)$ is decreased relative to that of $\epsilon_B(\lambda)$, as shown on Fig. 5. The crossover point of $\Delta A_{\parallel}$ will shift toward lower wavelength. For $\Delta A_{\perp}$ and ΔL the effect will be opposite: there is a shift between the three difference spectra.

One sees that all the information on $\Delta\theta$ is contained in the splitting of the crossover points of the difference spectra for the three types of measurements; hence the importance of comparing successive measurements on the same sample under the same conditions. This ensures that a difference in angular weight factor is measured and not the effects of distortions of the spectra by optical artifacts, since all the optics are common to the three measurements. As the information may be extracted not from the absolute positions of the crossover points, but from the difference between these positions, the result is rather insensitive to the exact shapes of the $\epsilon(\lambda)$. This was checked graphically by distorting these spectral shapes. Correlated to the changes of position of the crossover points there are also changes of amplitudes of the extrema of the difference spectra. Their quantitative exploitation is more delicate because they depend on the exact shapes of the $\epsilon(\lambda)$ and are more sensitive to spectral distortions. The sign of the splitting between the crossover points gives the sign of $\Delta\theta$ directly. The quantitative estimate of $\Delta\theta$ is obtained by simultaneously fitting the three difference curves and the crossover points by Eqs. 1, 2, and 3. The spectral shapes necessary for those fittings are extracted from our LD spectra. The comparison between only two measurements, $\Delta A_{\parallel}$ and $\Delta A_{\perp}$, is enough to estimate $\Delta\theta$. The linear dichroism measurement, which we obtained by a different technique on a sample of different concentration, provides two additional estimates independant from the first one.

Measurement of $\Delta\phi$

$\Delta\phi$ measurement was performed with axially oriented rods and axially polarized photoexcitation (geometry IV on Fig. 4). In the initial state, the rotationally symmetric distribution of rhodopsin dipoles around the beam direction gave no dichroism. LD was induced by photoselection. A 470-nm light polarized in the vertical direction photoexcited a small part of the total rhodo population and preferentially suppressed the rhodo having its dipole in the vertical direction. The remaining rhodo population had, therefore, a preferential orientation in the horizontal direction. This resulted in a negative LD amplitude in the wavelength range where rhodo absorbance predominates. This may as well be considered as the negative contribution of the suppressed rhodo population. The created batho population was also anisotropic: if there were no change of polar angle upon the transition ($\Delta\phi = 0$) the orientation of this created population would be vertical. Its LD, in the wavelength range where batho absorbance predominates, would be positive and maximal, e.g., that of a batho population selected by a perfect vertical polarizer without perturbation of the polar angle distribution. If $\Delta\phi \neq 0$, since one half of the disk membranes are observed from their cytoplasmic side and the other half from the intradiskal side, one half of the dipole population will be seen rotating clockwise, by $+\Delta\phi$ and the other half counter clockwise, by $-\Delta\phi$. This diminishes the anisotropy and therefore the LD amplitude. At the other extreme, if $\Delta\phi = \pi/2$ the batho population would be perfectly oriented in the horizontal direction, which would result in a negative LD amplitude in the wavelength range where bathorhodopsin absorbance predominates.

One sees qualitatively that the total photoinduced LD spectrum is a linear combination of the rhodo and batho specific absorbances $\epsilon_R(\lambda)$ and $\epsilon_B(\lambda)$, and that the relative coefficients depend on $\Delta\phi$; they are negative for $\Delta\phi = 0$ and positive for $\Delta\phi = \pi/2$.

The expression of ΔL_{PS} is given by Eq. 6. If $\Delta\phi$ is small this expression resembles that obtained for the difference spectra in the preceding section, but if $\Delta\phi > \pi/4$ the angular coefficients would have the same sign for $\epsilon_B(\lambda)$ and $\epsilon_R(\lambda)$ and the photoinduced LD spectrum would look like a sum spectrum instead of a difference spectrum.

In practice, the observed photoinduced LD has a wavelength-dependant shape analogous to that of the difference spectra of the preceding section, and the position of the crossover point is very close to that calculated using Eq. 6, indicating that $\Delta\phi$ is small. But this is only qualitative. Attempts to fit the shape of $LD_{PS}(\lambda)$ with linear combinations of $\epsilon_B(\lambda)$ and $\epsilon_R(\lambda)$, as required by Eq. 6, were unsuccessful; it was clear that the spectral shapes were distorted, as seen in Fig. 3.

This distortion resulted from a well-known artifact observed with particulate suspensions and termed "Duysens effect" or "sieve effect" (Duysens, 1956). This effect is due to the fact that the absorbing chromophores are not homogeneously dispersed in the solution but concentrated in particles of high optical density surrounded by transparent solution; the front part of a particle casts a shadow on the back part while light is allowed to pass without attenuation through the space existing between the particles. Although the average optical density of the sample, as recorded by the photomultiplier, may be very low, the chromophores in the back part of the particles receive much less light, and therefore absorb fewer photons than they would if the sample were homogeneous. The absorbance of the sample at a given wavelength is, therefore, reduced by a "flattening coefficient" which depends on the geometry of the particles and on their individual absorbance at this wavelength (Duysens, 1956; Gordon and Holzwarth, 1971). This effect, which distorts the absorbance peak shape, exists for any particulate suspension but is significant only when the optical density of the individual particles is large. While rods viewed transversally have a maximal optical density on the order of 10^{-1}, this optical density is close to 1 for a 50–60-μm long rod viewed axially. The sieve effect is, therefore, neglegible for transversally oriented rods. Furthermore this artifact would not change the position of the crossover points of the difference-absorbance spectra $\Delta A_{\parallel}$ and $\Delta A_{\perp}$, and would have very little effect on the crossover point of ΔL. But this sieve effect distorts significantly the absorbance and LD spectra of the axially oriented samples in the wavelength range where the absorbance of the individual rods is high.

To measure $\Delta\phi$, one must, therefore, devise a procedure, based entirely on the analysis of the induced LD amplitude in a spectral region of low absorbance. Such a procedure has been found; it is rather complex but is sensitive to small $\Delta\phi$ and is easy to check experimentally. It is based on the study of the rate of photoreversal by polarized light of the linear dichroism of a population of batho created by photoselection in the axially oriented rod sample. The measurements are made at a wavelength where only batho absorbs, so that the individual absorbance of the axially oriented rods is kept small when only a small proportion of the rhodo content of the rods is photoconverted.

When a batho population is created by photoexciting with vertically polarized light, this population is preferentially oriented in the vertical direction if $\Delta\phi$ is small. This population will therefore be more sensitive to photoreversal by vertically polarized light of the appropriate wavelength

than to the same amount of light polarized horizontally. The ratio of efficiencies of photoreversal for the two orthogonal directions of polarization depends on $\Delta\phi$ only (see Eq. 7). Following is the procedure:

(*a*) In an axially oriented sample of comparatively high concentration, a small photoselected population of batho is created by a short illumination with vertically polarized light of 472 nm.

(*b*) The amplitude of the photoinduced LD signal, ΔL_{PS} is measured at 600 nm, where only batho absorbs.

(*c*) The batho population is photoreversed by a sequence of small calibrated flashes of vertically polarized light of wavelength $\lambda > 605$ nm. The decrease of ΔL_{PS} (600) is plotted against the integrated photoreversal light intensity.

(*d*) The sample is fully photoreversed by unpolarized red light so that one returns to the initial state. The complete sequence is then repeated, but with horizontal polarization for photoreversal in (*c*).

Fig. 6 shows the evolution of $\Delta L_{PS}(600)$ in the function of the integrated photoreversal light intensities. The ratio of efficiency of photoreversal for the two orthogonal directions of polarization is maximum at the origin for $\Delta\phi = 0$, since this gives the maximal vertical orientation for the photoinduced batho population.

If $\Delta\phi$ is different from zero but small, there is an apparently paradoxal effect: photoreversal of batho by horizontally polarized light first increases LD_{PS}, and decreases it only upon higher integrated intensity, as shown in Fig. 6 *A*. This is due to the fact that the first effect of horizontally polarized light is to photoreverse preferentially the horizontal batho dipoles. As the vertical orientation is not perfect, this diminishes the dispersion of polar angle around the vertical, which was due to the $\Delta\phi$ rotation in the photoexcited transition. This increases the total anisotropy even though the total number of bathorhodopsin molecules is diminished: $A_\parallel - A_\perp$ increases because $A_\parallel$ decreases faster that $A_\perp$. With increased photoreversal light intensity, the whole population of batho is suppressed and the anisotropy decreases.

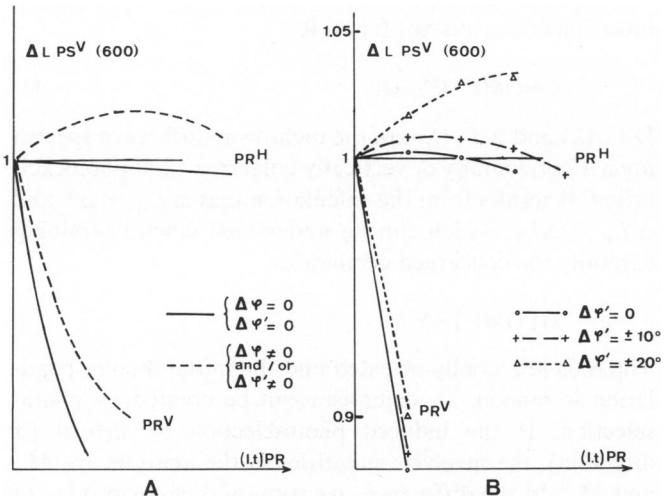

FIGURE 6 Measurement of the polar angle shift $\Delta\phi$ upon the rhodo-batho transition: ΔL^{v}_{PS} (600) is the amplitude of the linear dichroism peak of batho at 600 nm obtained upon a weak photoexcitation by vertically polarized light of wavelength 472 nm, on an axially oriented sample. A small proportion of the total rhodopsin population is photoconverted and the resulting ΔL^{v}_{PS} amplitude is normalized to 1. This photoselected batho population is then photoreversed by red ($\lambda > 605$ nm) light polarized either vertically (PR_v) or horizontally (PR_H). $(I.t)_{PR}$ denotes the integrated intensities of photoreversal light. The evolution of ΔL_{PS} upon this photoreversal depends only on $\Delta\phi$ (see text). *A*, schematics of the shape of photoreversal amplitude curves for $\Delta\phi = 0$ and for $\Delta\phi \neq 0$. (see text). *B*, experimental data, with perfect photoselection ($\Delta\phi' = 0$) and with artificial disorder $\pm\ \Delta\phi'$. Fitting the initial slopes $\delta_\parallel$ and $\delta_\perp$ of these photoreversal curves lead to estimate $\Delta\phi = 11 \pm 3°$.

The sensitivity of this effect of $\Delta\phi$ on the polarized photoreversal rates can be tested experimentally, by creating artificially an additional broadening in the photoselection process: in the photoexcitation step one rotates the polarizer by $+10°$, for example, with respect to the vertical direction during half the time of irradiation and by $-10°$ during the other half. If there were no $\Delta\phi$ this would be exactly equivalent to creating an artificial $\Delta\phi' = 10°$. If $\Delta\phi \neq 0$, $\Delta\phi'$ will combine with it and give an increased disorientation. But $\Delta\phi$ and $\Delta\phi'$ do not add up linearly, they must be convolved together. $\Delta\phi'$ gives a significant contribution and a sizeable change in the photoreversal behavior only if it is of the same order of magnitude as $\Delta\phi$. As soon as $\Delta\phi'$ becomes larger than $\Delta\phi$ its contribution becomes predominant. The sensitivity is, therefore, high around $\Delta\phi' = \Delta\phi$. Our experiments showed that $\Delta\phi$ is smaller than 20°, and the sensitive region is for $\Delta\phi'$ of the order of 10°. The quantitative estimate is not straightforward. It is based on fitting the curves of Fig. 6 using Eqs. 7, 8, and 9. But it is totally independent of $\Delta\theta$ and not very sensitive to the exact shapes of $\epsilon_B(\lambda)$ and $\epsilon_R(\lambda)$.

Additional Measurements, Sensitive to Both $\Delta\theta$ and $\Delta\phi$, and Checking the Geometry

A first type of measurement has been made in the geometry II of Fig. 4. This is the same geometry as for the $\Delta\theta$ measurement except that the photoexciting beam is polarized either vertically or horizontally. Starting in both cases from the same photoregenerated rhodopsin population (the photoregeneration is made with unpolarized light), two photoselected batho populations were obtained, which differed only by a rotation of $\pi/2$ of their preferential orientation axis. We measured the LD spectra before and after photoexcitation in both cases and from these obtained the two difference-LD spectra ΔL_V and ΔL_H and compared them. It is clear in this geometry that the vertically photoselected population will give a larger linear dichroism amplitude than the horizontally photoselected one, but the comparison bears on the shape of the difference spectra and particularly on the splitting between their crossover points, not on their amplitude. The splitting between ΔL_V and ΔL_H depends on both $\Delta\theta$ and $\Delta\phi$, as seen in Eqs. 4 and 5. $\Delta\theta$ is the dominating factor, which in our case shifts the crossover point of ΔL_H to longer wavelength than that of ΔL_V in the rhodo-batho conversion. The effect of $\Delta\phi$ is opposite: it tends to diminish the splitting due to $\Delta\theta$ as it tends to diminish the sharpness of the photoselection. If one accepts for $\Delta\theta$ the result already obtained in the first experiment described, which is very direct, the fit of the crossover splitting in this experiment provides a new and independant estimate of $\Delta\phi$.

A second type of measurement was made in the geometry III of Fig. 4; the transverse rods were photoexcited by an axial light which was polarized in the vertical or the horizontal direction. When the photoexciting beam was polarized in the vertical direction, the direction of the beam in the horizontal plane did not influence the probability of interaction with the dipole. The difference-LD spectrum upon vertical photoselection in this geometry must be identical to that observed in the preceding experiment with transverse light polarized vertically: $\Delta' L_V \equiv \Delta L_V$. The agreement between those two measurements with very different geometries of illumination provides an overall check on the precision of these geometries. It also indicates that depolarizing effects by light scattering, which could be feared in our samples upon transverse illumination, were negligible.

When the axial photoselecting beam is horizontally polarized, the direction of polarization is coaxial with the rod. Therefore the photoexcitation is isotropic around the rod axis and cannot induce any photoselection. The situation is analogous to that of geometry I, used for the measurement of $\Delta\theta$ and one must find $\Delta' L_H \equiv \Delta L$. This provides another check on the orientation of the sample and on the geometry of illumination and analysis.

It is clear in this last set of measurements with geometry III, that the photoregeneration must be performed with another light beam, transverse and unpolarized.

Useful Interpretative Formula

To estimate quantitatively the angular changes such as described in the previous section, the geometric factors weighing the spectral factors $\epsilon(\lambda)$ must be calculated from the knowledge of the photoexcitation and sample geometry described on Fig. 4.

The probability of interaction between a light beam polarized along the $\vec{p}$ direction and a dipole $\vec{u}$ (θ, ϕ) is proportional to their scalar square product and given by $(\vec{p} \cdot \vec{u})^2$. In $\vec{p}$ is included the photo excitation geometry and in $\vec{u}$ the retinal dipole spatial arrangement.

When a light beam polarized along the $\vec{i}$ direction is absorbed by a dipole $\vec{\mu}_R$, and induces for instance a rhodo $\rightarrow$ batho transition, that dipole becomes under the transition a dipole $\vec{\mu}_B$. If that new dipole is analyzed by a light beam polarized along the $\vec{j}$ direction the probability of interaction is proportional to $Mij = (\vec{i} \cdot \vec{\mu}_R)^2 \cdot (\vec{j} \cdot \vec{\mu}_B)^2$. Such quantities contain all the information concerning the spatial distribution of rhodopsin and bathorhodopsin dipole moments. They can be presented as a matrix M with elements Mij, in the reference frame $(\vec{x}, \vec{y}, \vec{z})$ where y is the rod axis direction, x and z are the horizontal and vertical directions (see Fig. 1).

$$M = \begin{bmatrix} \tfrac{1}{8}\sin^2\theta_R \sin^2\theta_B\,(1 + 2\cos^2\Delta\phi) & \tfrac{1}{2}\sin^2\theta_R\cos^2\theta_B & \tfrac{1}{8}\sin^2\theta_R \sin^2\theta_B\,(1 + 2\sin^2\Delta\phi) \\ \tfrac{1}{2}\cos^2\theta_R \sin^2\theta_B & \cos^2\theta_R\cos^2\theta_B & \tfrac{1}{2}\cos^2\theta_R \sin^2\theta_B \\ \tfrac{1}{8}\sin^2\theta_R \cos^2\theta_B\,(1 + 2\sin^2\Delta\phi) & \tfrac{1}{2}\sin^2\theta_R\cos^2{}_B & \tfrac{1}{8}\sin^2\theta_R \sin^2\theta_B\,(1 + 2\cos^2\Delta\phi) \end{bmatrix}$$

One extracts from M the quantities needed to calculate the shape of the difference spectra obtained in the different geometries upon various types of photoexcitation (see Fig. 4).

GEOMETRY I

The probability for the unpolarized photoexcitation to reach the $\vec{\mu}_R$ (θ_R, ϕ_R) species is independent of ϕ_R, and the created $\vec{\mu}_B$ (θ_B, ϕ_B) population is isotropic with respect to the rod axis and therefore independent of ϕ_B. This created population is analyzed in LD according to the specific absorbance of the μ_B species ϵ_B (λ) and to the difference of probabilities of absorption for a vertically and a horizontally polarized measuring light. In this simple case one can estimate directly from Fig. 1 that these probabilities are proportional to $\sin^2\phi_B \sin^2\theta_B$ and $\cos^2\theta_B$, respectively. After averaging over the random ϕ_B, the difference is $1/2\,(\sin^2\theta_B) - \cos^2\theta_B = (1 - 3\cos^2\theta_B)/2$. This LD is thus proportional to $[(1 - 3\cos^2\theta_B)/2]\ \epsilon_B\,(\lambda)$. In our notation, it is given by LD $= [\tfrac{1}{2}(M_{xz} + M_{zz}) - \tfrac{1}{2}(M_{xy} + M_{zy})]\ \epsilon(\lambda)$, which leads to the same formula.

The difference spectra ΔL, $\Delta A_\parallel$ and $\Delta A_\perp$, represent the contribution to the dichroism and absorption spectra, of this created population and the contribution of the "negative" population of rhodo which represents the depression of the initial state.

We normalize these difference spectra to the same amount of batho species (in the case of a rhodo $\rightarrow$ batho transition) to compare the shape of these spectra. For the geometry I of fig. 4,

$$\Delta L = \epsilon_B(\lambda) - \frac{1 - 3\cos^2\theta_R}{1 - 3\cos^2\theta_B}\epsilon_R(\lambda) \qquad (1)$$

$$\Delta A_\parallel = \epsilon_B(\lambda) - \frac{1 - \cos^2\theta_R}{1 - \cos^2\theta_B}\epsilon_R(\lambda) \qquad (2)$$

$$\Delta A_\perp = \epsilon_B(\lambda) - \frac{\cos^2\theta_R}{\cos^2\theta_B}\epsilon_R(\lambda). \qquad (3)$$

We emphasize that these quantities are unnormalized, and their consistency cannot be established unless the correct normalizing factor is put forward [e.g., $\Delta L = \Delta A_\parallel - \Delta A_\perp$ holds with $A_\parallel = (1 - \cos^2\theta/2)\ \epsilon(\lambda)$, $A_\parallel = \cos^2\theta \cdot \epsilon(\lambda)$ and LD $= (1 - 3\cos^2\theta/2)\ \epsilon(\lambda)$].

GEOMETRY II

Dichroism difference spectrum upon a vertically or horizontally polarized transverse photoexcitation in the absorption band of rhodopsin:

$$\Delta L_V = \epsilon_B(\lambda) - \frac{3 - 7\cos^2\theta_R}{(1 + 2\cos^2\Delta\phi)\,(1 - \cos^2\theta_B) - 4\cos^2\theta_B}\epsilon_R(\lambda) \qquad (4)$$

$$\Delta L_H = \epsilon_B(\lambda) - \frac{1 - 5\cos^2\theta_R}{(1 + 2\sin^2\Delta\phi)\,(1 - \cos^2\theta_B) - 4\cos^2\theta_B}\epsilon_R(\lambda). \qquad (5)$$

We can check with the right normalizations that $\Delta L = \Delta L_V + \Delta L_H$ For a reverse photoexcitation, in the absorption band of the batho, the same formulas hold with an inversion of the indexes B and R.

GEOMETRY III

$D'L_H(\lambda)$ and $\Delta'L_V(\lambda)$ are the dichroism difference spectra upon a horizontally or vertically polarized axial photoexcitation. It results from the calculation that $\Delta'L_H \equiv \Delta L$ and $\Delta'L_V = \Delta L_V$, which can be understood when examining carefully the concerned geometries.

GEOMETRY IV

The rods are axially oriented and the initial dipoles population is random. A dichroism can be created by photoselection. If the induced photoselection is vertical ($\vec{z}$ direction), the involved quantities in the analysis are M_{zz} and M_{zx}. In the difference spectrum of dichroism ΔL_{PS} of such an experiment, the quantities $M_{zz} - M_{zx}$ are weighted by each specific absorbance, leading to

$$\Delta L_{PS} = \sin^2\theta_B \cos(2\Delta\phi)\ \epsilon_B(\lambda) - \sin^2\theta_R\ \epsilon_R(\lambda). \qquad (6)$$

To obtain the efficiency of the photoreversal, which is polarized perpendicular or parallel to the photoexcitation, the probabilities of photoexcitation, photoreversion, and analysis in linear dichroism in the $\epsilon_B(\lambda)$ band are averaged over the dipoles' angular distribution. At first order and upon a perfectly polarized photoreversion, the variations of amplitude from the starting level ΔL_{PS} in the batho absorption range are found to be proportional to $\sin^2\Delta\phi$ for

a photoreversal light polarized perpendicularly to the photoselecting light and to $-\cos^2\Delta\phi$ for a photoreversal light parallel to the photoselecting light. In Fig. 6, where those amplitudes are provided, the initial slopes for the two directions of photoreversal polarization are given by:

$$\delta_{\parallel} = \sin^2\Delta\phi$$
$$\delta_{\perp} = -\cos^2\Delta\phi. \quad (7)$$

If the photoselection is oriented at angle $\Delta\phi'$ from the vertical, a population is created that is photoselected and depressed and is analyzed as

$$\Delta L'_{PS} = \sin^2\theta_B \cos(2\Delta\phi)\cos(2\Delta\phi')\,\epsilon_B(\lambda) - \sin^2\theta_R \cos(2\Delta\phi')\,\epsilon_R(\lambda) \quad (8)$$

The amplitude of the LD in the $\epsilon_B(\lambda)$-band is proportional to $\cos(2\Delta\phi)\cos(2\Delta\phi')$ instead of $\cos(2\Delta\phi)$ for a perfectly polarized vertical photoselection ($\Delta\phi' = 0$). To evaluate the photoreversal efficiency we represent the effect of a $\Delta\phi' \neq 0$ term by the symbolic addition $\Delta\phi \oplus \Delta\phi' = \Delta\phi^*$, such that

$$\cos(2\Delta\phi)\cos(^2\Delta\phi') = \cos(2\Delta\phi^*) \quad (9)$$

$\Delta\phi^*$ is then used in Eqs. 7 giving the efficiency of the photoreversal.

RESULTS

Measurements of $\Delta\theta$

Linear dichroism spectra of transversally oriented samples are shown in Figs. 7 and 8, for pure rhodo and iso states, and for photoequilibrium mixtures of rhodo, iso, batho, and lumi. Difference absorbance and LD spectra for the corresponding transitions are shown on Figs. 9 and 10. The positions of the crossover points of these difference spectra are listed on Table I for all the transitions studied.

The estimates of $\Delta\theta$ are based on the fitting of the difference spectra and in particular of their crossover points, by Eqs. 1–3. Taking as an example the rhodo → batho transition, one sees that one needs to know three parameters, $\epsilon_B(\lambda)$, $\epsilon_R(\lambda)$, and θ_R, to extract the fourth one, θ_B, and therefore $\Delta\theta_{RB}$. One gets directly the shape of $\epsilon_R(\lambda)$ from the LD spectrum of pure rhodopsin (Fig. 7), but $\epsilon_B(\lambda)$ has to be reconstructed, as this species appears only in photoequilibrium mixtures. From the knowledge of $\Delta A_{\parallel}$ and $\Delta A_{\perp}$ with their proper relative normalization one can, by linear interpolation, build the difference spectrum ΔA proportional to $\epsilon_B(\lambda) - \epsilon_R(\lambda)$ and independent of the angular factors.

Linear combinations of $\epsilon_R(\lambda)$ and ΔA lead then to simultaneous estimates of a shape for $\epsilon_B(\lambda)$, a ratio $\epsilon_B(\lambda\text{max})/\epsilon_R(\lambda\text{max})$, and a percentage of batho in the photoequilibrium mixture. Optimizing these three parameters with respect to the data existing in the literature (Oseroff and Callender, 1974, Eyring and Mathies, 1976, Kawamura et al., 1977, Aton et al., 1980, Mao et al., 1980), we obtain $\epsilon_B(\lambda)$ at the same scale as $\epsilon_R(\lambda)$, with the very satisfactory set of parameters listed in Tables II and III. Table III shows that the λ_{max} for rhodopsin is slightly higher than that given by Kawamura et al. (1977) for equivalent frog rod suspensions at liquid nitrogen temperature. We notice, however, in a later publication of the same group (Kawamura et al., 1978) that the λ_{max} for rhodopsin in a spectrum shown is close to 520 nm, in agreement with our data.

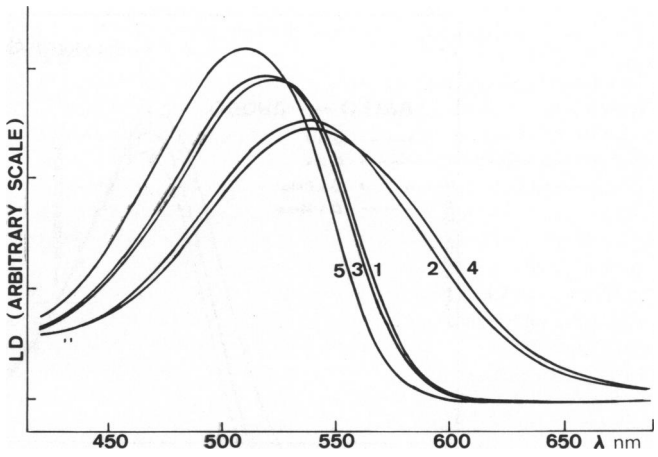

FIGURE 7 Linear dichroism spectra of transversally oriented rods at liquid nitrogen temperature. Spectrum *1* is the initial spectrum of a dark adapted sample. Spectrum *2* is obtained after nonsaturating transverse illumination with unpolarized light of 472 nm. Spectrum *3* is obtained after saturating illumination at 472 nm followed by photoreversal by light of $\lambda > 605$ nm. It contains an admixture of ~25% iso. Spectrum *4* is obtained upon further saturating illumination at 472 nm. *3* and *4* are the two photoequilibra obtained upon sequential saturation with light of $\lambda >$ 605 nm and light of 472 nm. Spectrum *5* is obtained on prolonged illumination with light of $\lambda > 580$ nm.

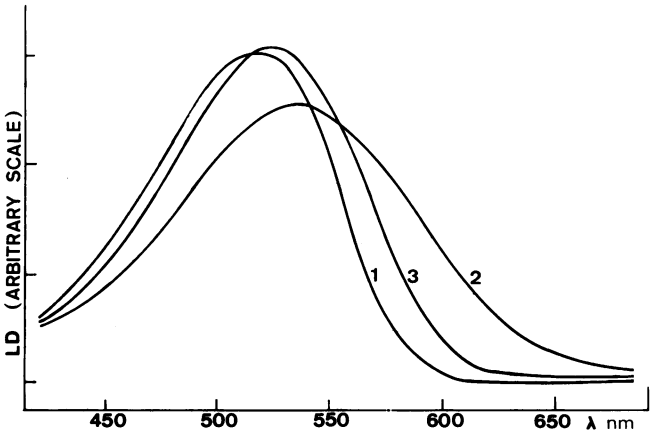

FIGURE 8 Linear dichroism spectra of transversally oriented rods at liquid nitrogen temperature. Spectra *1* and *2* are equivalent, respectively, to spectra *3* and *4* on Fig. 7. Spectrum *3* is obtained by letting the sample warm up to −110°C for 30 min after saturating illumination with λ = 472-nm light. The sample is then cooled back to liquid nitrogen temperature.

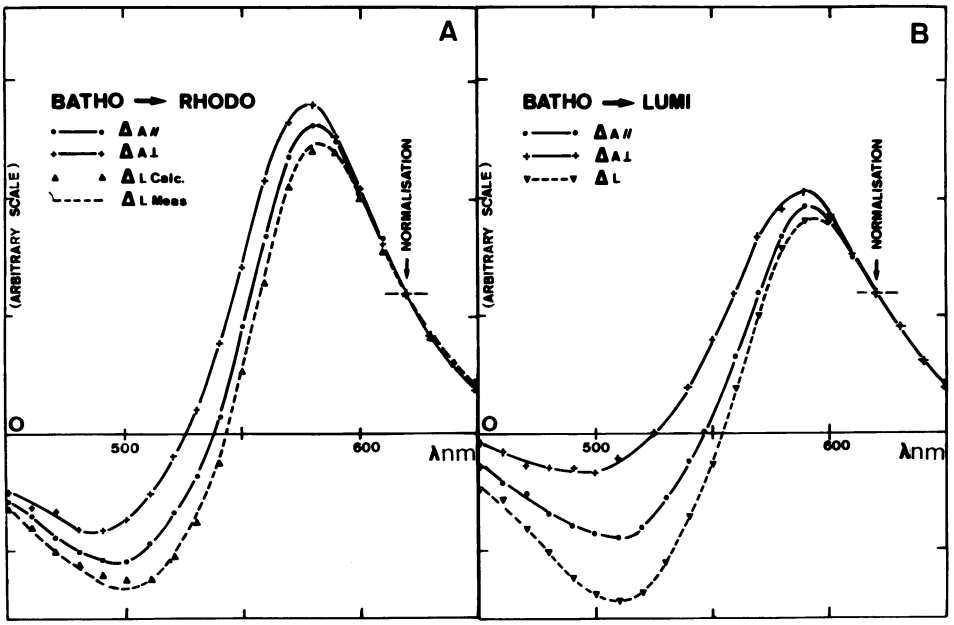

FIGURE 9 Difference-polarized absorbance spectra $\Delta A_{\parallel}$ and $\Delta A_{\perp}$, and difference-linear dichroism spectra ΔL upon the batho → rhodo transition (A) and upon the batho → lumi transition (B) on a transversally oriented sample at liquid nitrogen temperature (geometry I). In A the photoequilibrium obtained by illuminating rhodopsin at 472 nm was photoreversed by light of wavelength > 605 nm. There is a 20% admixture of batho → iso transition in this photoreversal process. In B the same photosteady state was allowed to warm up to −110°C for 30 minutes and cooled back down to liquid nitrogen temperature. All the difference spectra have a common normalization at 620 nm where only batho absorbs. The fact is emphasized that their shapes are all described by expression of the type $\epsilon_B(\lambda) - k(\theta)\,\epsilon_R(\lambda)$ (see Fig. 5). If the spectral shapes are not distorted, they must overlap in the wavelength range >600 nm where only Batho absorbs. The excellent agreeement between $\Delta(A_{\parallel} - A_{\perp})$ calculated from the polarized absorption measurements on a sample of high concentration ($A_{500} \simeq 0.3$), and ΔL measured directly in the dichrograph on a sample of low concentration ($A_{500} \simeq 0.03$) indicates that there is in this geometry no concentration-dependant spectral distortion. The relative dispositions of the difference spectra and of their cross over points demonstrate unambiguously that in A, $\theta_R > \theta_B$ and in B, $\theta_L > \theta_B$. Quantitative estimates of $\Delta\theta_{RB}$ and $\Delta\theta_{BL}$ are obtained from the simultaneous fitting of the difference spectra (see Fig. 11). Although the shifts between the difference spectra are larger in B than in A, they correspond to approximately identical angular shifts in both transitions.

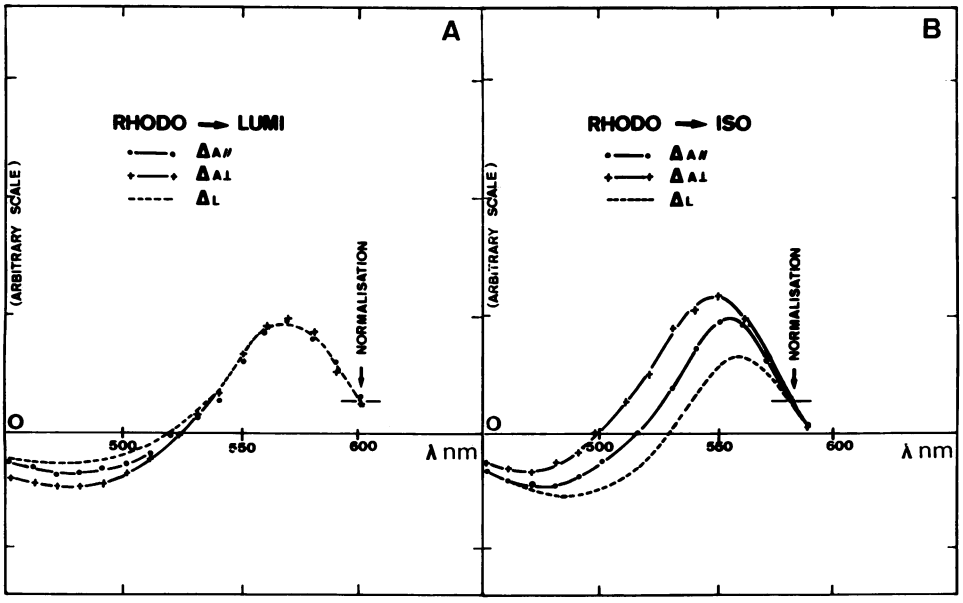

FIGURE 10 Difference-polarized absorbance and linear dichroism spectra on transversally oriented samples at liquid nitrogen temperature. In A the maximum conversion to iso is obtained by prolonged illumination with light of wavelength >580 nM. In B lumi is obtained by illuminating with 472-nm light and letting the sample warm up at −110°C for 30 min. In both cases the difference amplitudes are small because the spectral shapes of rhodo, iso and lumi are very close to each other. The common normalization is not very reliable for the same reason, as there is no large range where one species only absorbs. The shifts between the crossover points are very sensitive to the angular factors as the spectral shapes are close: in A the large shift observed corresponds to an angular shift $\Delta\theta_{RI} < 1°$. In B the shifts are very small and correspond to an estimate of $\Delta\theta_{RL}$ not significantly different from zero.

TABLE I
WAVELENGTH OF THE CROSSOVER POINTS OF THE DIFFERENCE ABSORBANCE AND LINEAR DICHROISM SPECTRA FOR THE VARIOUS TRANSITIONS*

	$\Delta A_{\perp}$	$\Delta A_{\parallel}$	ΔL
		nm	
rhodo → batho	528 ± 1	538 ± 1	544 ± 1
batho → rhodo + 20% Iso	527 ± 1	536 ± 1	542 ± 1
rhodo → iso	497 ± 4	514 ± 2	528 ± 1
batho → iso	517 ± 1	530 ± 1	537 ± 1
batho → lumi	525 ± 2	546 ± 2	554 ± 1
rhodo → lumi	522 ± 3	517 ± 3	513 ± 3

*Transitions were measured on transversally oriented samples (geometry I), at liquid nitrogen temperature.

Once $\epsilon_B(\lambda)$ and $\epsilon_R(\lambda)$ are obtained, the fits depend only on the angles θ_R and θ_B. Taking $\theta_R = 72°$ as the best estimate from the literature (Liebman, 1962, 1972, Wald et al., 1963, Harosi, 1975) the fit of the three difference spectra, is obtained for $\theta_B = 69°$; that is $\Delta\theta_{RB} = -3°$. Slight variations of θ_R around the accepted value gives comparable variations of θ_B, but very little change of $\Delta\theta_{RB}$. Similarly, small changes of shape and amplitude of $\epsilon_R(\lambda)$ and $\epsilon_B(\lambda)$ have very little influence on the estimate of $\Delta\theta$ as long as one requires the simultaneous fitting of the three crossover points of $\Delta A_{\parallel}$, $\Delta A_{\perp}$, and ΔL.

We have also from our own data a direct estimate of θ_B. This is obtained from the ratio of absorbances $A_{\parallel B}/A_{\perp B} = \frac{1}{2} tg^2\theta_B$ (see Liebman, 1962), in the wavelength range where only batho absorbs. The measurement is made feasible by the fact that the base-line absorbance level can be measured without moving the sample after photoreversing batho to rhodo. We got $A_{\parallel B}/A_{\perp B} = 2.44 \pm 0.04$ which leads to $\theta_B = 65.5 \pm 0.5°$. This can be only an underestimate, as any imperfection in the sample orientation can only diminish the ratio. Taking then $\theta_B = 66°$, the fitting of the crossover points of $\Delta A_{\parallel}$ and $\Delta A_{\perp}$ and ΔL leads to $\theta_R = 69°$ (Fig. 11) which gives again $\Delta\theta_{RB} = -3°$, in agreement with what was said above on the insensitivity of the $\Delta\theta$ estimate on the exact value of θ_R.

Similar procedures were used for all the transitions studied, and the set of $\Delta\theta$ evaluations are shown in Fig. 12. The results are redundant in the sense that, the result of the direct rhodo-lumi comparison is independent from that of the rhodo-batho and batho-lumi transitions. The agreement between those independent estimates give a high degree of confidence in our results (see Fig. 11).

TABLE II
WAVELENGTH OF MAXIMUM ABSORBANCE, AND MAXIMUM ABSORBANCE NORMALIZED WITH RESPECT TO RHODOPSIN

	λ_{max}	ϵ_{max}
Rhodo	522 ± 2	1
Batho	570 ± 3	1.27 ± 0.05
Iso	510 ± 2	1.09 ± 0.02
Lumi	530 ± 2	1.03 ± 0.02

Wavelengths were measured or estimated from our linear dichroism spectra at liquid nitrogen temperature.

TABLE III
PHOTOEQUILIBRIUM MIXTURE OBTAINED UPON THE VARIOUS SEQUENCES OF SATURATING ILLUMINATION

Sequence of saturating light	Rhodo	Iso	Batho
(nm)		%	
λ = 472 + λ > 605	75	25	0
λ = 472 + λ > 605 + λ = 472	29	13	58
λ > 580	0	>95	0

The percentages are accurate to within 5%.

Measurements of $\Delta\phi$

The complete $\Delta\phi$ measurement has been performed only for the rhodo → batho transition. The procedure is described in the Material and Methods section. The photoinduced LD spectrum on an axially oriented sample

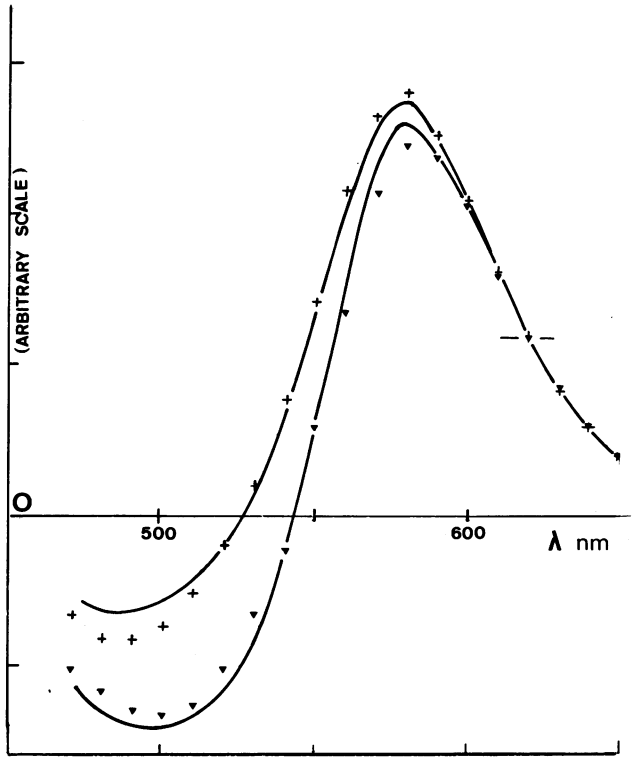

FIGURE 11 Example of simultaneous fits of two difference spectra $\Delta A_{\perp}$ (+) and ΔL (▼) for the batho → rhodo transition (see Fig. 8 *A*). These fits were obtained using a batho absorbance spectrum having its maximum at 570 nm and $\epsilon_B(max) = 1.27\ \epsilon_R(max)$. Taking $\theta_B = 66°$ (our experimental estimate) one gets for fitting the crossover regions $\theta_R = 68.6$; that is $\Delta\theta_{RB} = -2.6°$. When the fixed value for θ_B (or θ_R) is varied lightly, e.g. taking $\theta_R = 72°$, the simultaneous fitting of the crossover regions is consistently obtained for values of $\Delta\theta_{RB}$ of the order of $-3°$. Changing the shape $\epsilon_B(\lambda)$ [or $\epsilon_R(\lambda)$] slightly, changes only the quality of the fit around the extrema but not the estimate of $\Delta\theta_{RB}$.

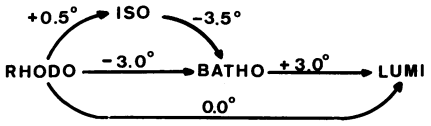

FIGURE 12 The azimuthal angle changes $\Delta\theta$ upon the various transitions. The uncertainties in this results are estimated to ±0.5°. The different branches have been measured independantly and the data are redundant, and consistent.

is shown on Fig. 3 and the polarized photoreversal rates curves are plotted in Fig. 6, with that obtained when adding an artificial disorder in the photoselection: $\Delta\phi' = \pm 10°$ and $\Delta\phi' = \pm 20°$.

Using Eq. 7, we extracted from each of the three measurements the estimates $\Delta\phi = 8°$, $\Delta\phi^*_{10} = 14°$, and $\Delta\phi^*_{20} = 23°$ from the measured ratios $(\delta_\parallel/\delta_\perp)$ of the initial photoreversal slopes. When the contribution of $\Delta\phi'$ is extracted from $\Delta\phi^*$, one gets three independent estimates for $\Delta\phi$: 8°, 10°, and 12.5°. Taking into account the various uncertainties, our best estimate was $\Delta\phi = 11° \pm 3°$.

As a check on this estimate we performed the "additional measurement" with geometry III (see Material and Methods), which is sensitive to both $\Delta\theta$ and $\Delta\phi$. We found, for the rhodo → batho transition, a splitting between the crossover points of ΔL_V and ΔL_H, which were located at 540 nm and 545 nm, respectively.

Using Eqs. 4 and 5 and inserting our measured value of $\Delta\theta$, we estimated $\Delta\Phi \simeq 14°$. This value is an upper limit, all disorienting factors tending to decrease the crossover splitting. It is, therefore, in excellent agreement with the previous and totally independent estimation.

The same experiment with Geometry III was also performed for the iso → batho transition. A splitting was also measured between ΔL_V and ΔL_H, located at 534 and 538 nm, respectively. This is a rough indication that $\Delta\phi$ is of the same order of magnitude when reaching batho either from rhodo or from iso. It suggests that the geometry of the dipole in the iso state is very close to that in native rhodopsin.

DISCUSSION

The overall angular change of the dipole of retinal upon the rhodo → batho transition is easily calculated when θ_R (or θ_B), $\Delta\theta$ and $\Delta\phi$, are known. Taking $\theta_R = 72°$ as the best estimate, from our measured $\Delta\theta = 3°$ and $\Delta\phi = 11 \pm 3°$ we deduce $\Delta\Omega = 10.8 \pm 2.7°$, which we round up to $\Delta\Omega = 11 \pm 3°$. Our result confirms, therefore, that a significant reorientation occurs upon the transition. This is indicative of a geometric change in the conformation of the chromophore and makes it unlikely that the rhodo–batho transition reflects only a phenomenon such as a charge transfer along a chromophore of fixed geometry.

The main component of the angular shift appears to be in the membrane plane. This may be correlated to the orientation of the approximate symetry plane of the 11-*cis* retinal molecule in rhodopsin, as defined by the two dipoles corresponding to the α and β-bands in the visible spectrum (Sperling and Rafferty, 1969, Kakitani and Kakitani, 1978). Microspectroscopic measurements (Liebman, 1973, Harosi, 1975) confirmed by our recent measurements on oriented rods (Chabre and Breton, 1979) have shown that the β-band has a dichroic ratio comparable to that of the α-band, indicating that the β-dipole is also inclined towards the membrane plane. The plane of symetry of the 11-*cis* retinal molecule is, therefore, nearly parallel to the membrane plane. With such an initial geometry it is clear that upon a *cis-trans* isomerisation the rotation of the dipole direction should have its major component in the membrane plane; that is, in $\Delta\phi$, and only a minor azimuthal component, $\Delta\theta$.

The amplitude that we measure for the angular shift of the α-dipole upon the rhodo-batho transition is, however, much smaller than might have been expected from a simplistic picture of the transition between undistorted 11-*cis* and all-*trans* conformations of retinal chromophore having a fixed β-ionone end. Comparing simply the polyene chain geometry in both conformations one estimates an angular shift of ~28°, which is almost exactly what has been measured by the Yoshizawa group (Kawamura et al., 1979). Evidence has been accumulated to demonstrate that the conformation of the chromophore is distorted in the initial rhodo state as well as in the batho state (e.g., Honig et al., 1979, Eyring et al., 1980). Furthermore, the binding site in opsin is not very tight. It is well known that 9-*cis* and 9–13-*cis* isomers of retinal are accepted easily as a substitute to form viable rhodopsin. But, even around the β-ionone end, the site seems to be lenient: it has recently been demonstrated (Blatchy et al. 1980) that opsin can accomodate analogue of retinal with very bulky substitutes for the β-ionone ring. The conformation of the chromophore is highly strained in batho, as demonstrated by the large energy uptake in the first step (Cooper, 1979). According to Honig et al. (1979) most of the energy storage arises from the displacement of the Schiff bond end, which separates an ion pair. Because the chromophore must be tightly fixed to stand the strain, one may imagine that upon the isomerization, both ends of the chromophore move, the β-ionone end as well as the Schiff-base bonded end, so that the overall movement of the polyene chain would be minimized. Warshel (1976) has also proposed isomerization mechanisms in which the molecular motion of the chromophore is very restricted. But these restricted movements of the chromophore are not absolutely required by our results; if one accepts the fact that the all-*trans* conformation is twisted in batho, the absorbing dipole in this twisted conformation may no longer be strictly aligned with the polyene chain. Even with a fixed chromophore, in which only the Schiff-base end would move, the orientational change of the dipole in the rhodo → batho transition may then be smaller than that expected for a transition from a planar *trans* to a

planar *cis* conformation. Theoretical estimates of the orientation of the absorbing dipole in a twisted conformation are still missing.

Our results for the rhodo–batho transition do not agree with that of the only other published experimental study, that of Yoshizawa's group (Tokunaga et al., 1976, Kawamura et al., 1977, 1978, 1979). These authors found for θ, instead of the small decrease we observe, a large increase, of the order of 20°, so that the chromophore in batho would lie exactly in the membrane plane. For ϕ they also found a change of the order of 20°, this combining to give an overall shift $\Delta\Omega = 26°$. We think the origin of the discrepancy for $\Delta\theta$ may lie in the neglect in their analysis of the sieve effect for the absorbance measurements on retinas.

Their method is based on the comparison of absorbance spectra of retinas to that of unoriented rod samples or solubilized rhodopsin which are not affected at the same level by the sieve effect. Our own experience is that a straight comparison of the difference absorbance spectra of axial samples to that of transversally oriented, or unoriented, samples would have led us to a result close to theirs. But the various difference spectra would not be fitted with a unique spectral shape for rhodopsin and/or batho. One notices, in fact, in the analysis of Kawamura et al. (1977), that the spectral shape of batho for the retina is quite different from that obtained with rod suspensions (their Fig. 3). This cannot arise from an angular change of the chromophore, which would change the normalization factors but not the spectral shapes.

For $\Delta\phi$ we think the large value obtained by Kawamura et al. (1979) might result from an underestimation in their analysis of the decrease of photoselection efficiency upon long illuminations. Photoselection is perfect only at the limit where the photoselected population is neglegible compared with the initial population. Indeed, we notice that the $\Delta\phi$ estimate they would obtain with very short illumination time (their Fig. 5) would be lower and compatible with our own result.

In the batho-lumi decay, we find, in agreement with Kawamura et al., that the θ-angle of the chromophore shifts back almost exactly to its original value in rhodopsin. Our method also allows a direct comparison of the θ-angle of lumi and rhodo, which confirms that the azimuthal change is very small between those two states. We cannot state, however, that the chromophore orientation has shifted back to its original position, since we did not measure the evolution of the polar angle ϕ in lumi. The θ-angle has already been measured for the later states of the decay, Meta I, Meta II and Meta III (Chabre and Breton, 1979). Except for Meta II this azimutal angle remains very close to that in rhodopsin. The major changes in the geometry of the chromophore in the protein seem, therefore, to be correlated to two important transitions: the initial transition to batho, when the isomerization occurs, and the late Meta I → Meta II transition, where major changes occur in the protein and in the binding between the chromophore and the protein.

We wish to thank Mr. C. Gagne for his contribution in the design and setting up of the dichrograph. We thank Dr. G. Maret and the staff of the Service National des Champs Intenses for the very easy and efficient use of the high field magnet.

This work was supported in part by a contract from the Délégation Générale à la Recherche Scientifique et Technique, Comité des Membranes Biologiques.

Received for publication 9 May 1981 and in revised form 28 August. 1981.

REFERENCES

Aton, B., A. G., Doukas, D. Narva, R. H. Callender, U. Dinur, and B. Honig. 1980. Resonance Raman studies of the primary event in visual pigment. *Biophys. J.* 29:79–94.

Blatchy, R., J. D. Carriker, V. Balogh-Nair, K. N. Nakanisht. 1980. Adamantyl allenic rhodopsin. Leniency of the ring binding site in bovine opsine. *J. Am. Chem. Soc.* 102:2495–2497.

Breton, J., M. Michel-Villaz, and G. Paillotin. 1973. Orientation of pigments and structural proteins in the photosynthetic membrane of spinach chloroplast: a linear dichroism study. *Biochim. Biophys. Acta.* 314:42–56.

Chabre, M. 1975. X-ray diffraction study of retinal rods. *Biochim. Biophys. Acta.* 382:322–335.

Chabre, M., and J. Breton. 1979. The orientation of the chromophore of rhodopsin in the "Meta" intermediate states, and the reversibility of the Meta II-Meta III transition. *Vision Res.* 19:1005–1018.

Cooper, A. 1979. Energy uptake in the first step of visual excitation. *Nature (Lond.).* 282:531–533.

Duysens, L. N. M. 1956. The flattening of the absorption spectrum of suspensions, as compared to that of solutions. *Biochim. Biophys. Acta.* 19:1–20.

Eyring, G., B. Curry, R. Mathies, R. Fransen, I. Paling, and J. Lugtenburg. 1980. Interpretation of the resonance Raman spectrum of Bathorhodopsin based on visual pigment analogues. *Biochemistry.* 19:2410–2418.

Gordon, D. J., and G. Holzwarth. 1971. Artifacts in the measured activity of membrane suspensions. *Arch. Biochem. Biophys.* 142:481–488.

Green, B. H., T. G. Monger, R. R. Alfano, B. Aton, and R. H. Callender. 1977. *Cis-trans* isomerisation in rhodopsin occurs in picoseconds. *Nature (Lond.).* 269:179–180.

Harosi, F. I. 1975. Absorption spectra and linear dichroism of some amphibians photoreceptors. *J. Gen. Phys.* 66:357–382.

Honig, B., T. Ebrey, R. H. Callender, U. Dinur, and M. Ottolenghi. 1979. Photo-isomerisation, energy storage and charge separation. A model for light energy transduction in visual pigment and bacteriorhodopsin. *Proc. Natl. Acad. Sci. U.S.A.* 76:2503–2507.

Hubbard, R., and A. Kropf. 1958. The action of light on rhodopsin. *Proc. Natl. Acad. Sci. U.S.A.* 44:130.

Kakitani, T. and H. Kakitani. 1976. Molecular mechanism for the initial process of visual excitation. *Biophys. Struct. Mech.* 5:55–73.

Kawamura, S., F. Tokunaga, and T. Yoshizawa. 1977. Absorption spectra of rhodopsin and its intermediates and orientationnal change of the chromophore. *Vision Res.* 17:991–999.

Kawamura, S., S. Wakabayashi, A. Maeda, and T. Yohizawa. 1978. Isorhodopsin. Conformation and orientation of its chromophore in frog disk membranes. *Vision Res.* 18:457–462.

Kawamura, S., F. Tokunaga, T. Yoshizawa, A. Sarai, and T. Takikani. 1979. Orientationnal changes of the transition dipole moment of retinal chromophore on the disk membrane due to the conversion of rhodopsin to bathorhodopsin and isorhodopsin. *Vision Res.* 19:879–884.

Liebman, P. A. 1962. *In situ* microspectrophotometric studies on the pigment of single retinal rods. *Biophys. J.* 2:161–178.

Liebman, P. A. 1972. Microspectrophotometry of photoreceptors. *In* Handbook of Sensory Physiology. Photochemistry of Vision. H. J. A. Dartnall, editor. Springer Verlag, Berlin. Vol. VII/I 481–528.

Mao, B., T. G. Ebrey, and R. Crouch. 1980. Batho products of rhodopsin, isorhodopsin I, and isorhodopsin II. *Biophys. J.* 29:247–256.

Oseroff, A. R., and R. H. Callender. 1974. Resonance Raman spectroscopy of rhodopsin in retinal disk membranes. *Biochemistry.* 13:4243–4248.

Peters, K., M. L. Appelbury, and P. M. Rentzepis. 1977. Primary photochemical event in vision: proton translocation. *Proc. Natl. Acad. Sci. U. S. A.* 74:3119–3123.

Sperling, W., and C. N. Rafferty. 1969. Relationship between absorption spectrum and molecular conformation of 11-*cis* retinal. *Nature (Lond.).* 224:591–594.

Tokunaga, F., S. Kawamura, and T. Yoshizawa. 1976. Analysis by spectral difference of the orientational change of the rhodopsin chromophore during bleaching. *Vision Res.* 16:633–641.

Wald, G., P. K. Brown, and I. R. Gibbons. 1963. The problem of visual excitation. *J. Opt. Soc. Am.* 53:20–35.

Warshel, A. 1976. Bycicle-pedal model for the first step in the vision process. *Nature (Lond.).* 260:679–683.

Yoshizawa, T. and G. Wald. 1963. Prelumirhodopsin and the bleaching of visual pigment. *Nature (Lond.).* 197:1279–1286.